JOURNAL OF NEUROTRAUMA 36:2246–2259 (July 15, 2019)

DOI: 10.1089/neu.2018.6266

Testosterone Administration after Traumatic Brain Injury Reduces Mitochondrial Dysfunction and Neurodegeneration

Randhall B. Carteri,[1] Afonso Kopczynski,[1] Marcelo Salimen Rodolphi,[1] Nathan Ryzewski Strogulski,[1] Mônia Sartor,[1] Marceli Feldmann,[1] Marco Antonio De Bastiani,[1] Clovis Milton Duval Wannmacher,[1,2] Itiane Diehl de Franceschi,[1,2] Gisele Hansel,[3] Douglas H. Smith,[3] and Luis Valmor Portela[1]

Abstract

Traumatic brain injury (TBI) increases Ca^{2+} influx into neurons and desynchronizes mitochondrial function leading to energy depletion and apoptosis. This process may be influenced by brain testosterone (TS) levels, which are known to decrease after TBI. We hypothesized that a TS-based therapy could preserve mitochondrial neuroenergetics after TBI, thereby reducing neurodegeneration. C57BL/6J mice were submitted to sham treatment or severe parasagittal controlled cortical impact (CCI) and were subcutaneously injected with either vehicle (VEH-SHAM and VEH-CCI) or testosterone cypionate (15 mg/kg, TS-CCI) for 10 days. Cortical tissue homogenates ipsilateral to injury were used for neurochemical analysis. The VEH-CCI group displayed an increased Ca^{2+}-induced mitochondrial swelling after the addition of metabolic substrates (pyruvate, malate, glutamate, succinate, and adenosine diphosphate [PMGSA]). The addition of Na^+ stimulated mitochondrial Ca^{2+} extrusion through $Na^+/Ca^{2+}/Li^+$ exchanger (NCLX) in VEH-SHAM and TS-CCI, but not in the VEH-CCI group. Reduction in Ca^{2+} efflux post-injury was associated with impaired mitochondrial membrane potential formation/dissipation, and decreased mitochondrial adenosine triphosphate (ATP)-synthase coupling efficiency. Corroborating evidence of mitochondrial uncoupling was observed with an increase in H_2O_2 production post-injury, but not in superoxide dismutase (SOD2) protein levels. TS administration significantly reduced these neuroenergetic alterations. At molecular level, TS prevented the increase in $pTau^{Ser396}$ and alpha-Spectrin fragmentation by the Ca^{2+}dependent calpain-2 activation, and decreased both caspase-3 activation and Bax/BCL-2 ratio, which suggests a downregulation of mitochondrial apoptotic signals. Search Tool for the Retrieval of Interacting Genes/Proteins database provided two distinct gene/protein clusters, ''upregulated and downregulated,'' interconnected through SOD2. Therefore, TS administration after a severe CCI improves the mitochondrial Ca^{2+}extrusion through NCLX exchanger and ATP synthesis efficiency, ultimately downregulating the overexpression of molecular drivers of neurodegeneration.

Key words: mitochondria; neurodegeneration; neuroenergetics; testosterone; traumatic brain injury

Introduction

Now recognized as a major health disorder, traumatic brain injury (TBI) commonly results in persisting neurological dysfunction.[1,2] The initial pathophysiological changes resulting from primary mechanical damage can trigger secondary deleterious effects, including progressive neurodegeneration.[3] However, the cellular and molecular mechanisms involved in these progressive changes are poorly understood.[4,5] Nonetheless, it has been suggested that persisting metabolic dysfunction may underlie some of the pathological features of chronic TBI.

In experimental TBI, mitochondrial dysfunction has commonly been described as a source of cellular metabolic crisis.[6,7] This is thought to reflect, in part, pathological increases in intracellular calcium (Ca^{2+}) concentrations, which in turn is sequestered by the mitochondria. However, this buffering of calcium comes at a cost of a decreased capacity of mitochondria to generate adenosine triphosphate (ATP). The resultant hypometabolism may desynchronize cell function concomitant with a rise in reactive oxygen species.[8,9] With increases in Ca^{2+} exceeding the capacity of mitochondrial sequestration, proteases such as calpain are activated, causing chemical destruction of the cytoskeleton, which can ultimately lead to cell death.[10]

The entrance of Ca^{2+} in the mitochondrial matrix is mediated through the mitochondrial calcium uniporter, which imports Ca^{2+} across the inner membrane partially, thereby dissipating the mitochondrial membrane potential ($\Delta\Psi_m$). In contrast, the mitochondrial sodium–calcium-lithium exchanger (NCLX), balances Ca^{2+}

[1]Laboratory of Neurotrauma and Biomarkers, [2]Department of Biochemistry, Federal University of Rio Grande do Sul, Porto Alegre, Brazil.
[3]Penn Center for Brain Injury and Repair and Department of Neurosurgery, University of Pennsylvania, Philadelphia, Pennsylvania.

influx by extruding one Ca^{2+} ion in exchange for three sodium ions (Na^{+}).[11] Further, the NCLX is proposed to be responsible for mitochondrial Ca^{2+} extrusion in excitable cells like neurons. Thus, it has been proposed that TBI primes neurons to die due to the confluence of mitochondrial dysfunction and subsequent degenerative processes.[12] Indeed, there has been substantial interest in pharmacologically targeting deleterious pathways in mitochondria after TBI. [9,13,14]

Testosterone (TS) is a gonadal hormone that improves brain glucose metabolism, synaptic plasticity,[15] antioxidant defenses, neurogenesis, and cell survival after different *in vitro* and *in vivo* injury models[16] via reductions of pro-apoptotic stimuli.[17] In contrast, decreased TS levels in castrated rats caused perturbations in the hippocampal mitochondrial genes involved in the electron transport system, biogenesis, and oxidative metabolism. However, these processes were recovered soon after the androgen replacement therapy was initiated. Hence, at least in part, the benefits of TS therapy on the brain likely involves direct effects on mitochondrial function.[18] Noteworthy, mice brain TS levels inversely correlate with edema formation and neurological deficits after TBI.[19] Additionally, adult TBI patients are susceptible to acute perturbations in the pituitary function, namely post-traumatic hypopituitarism,[20,21] leading to hypogonadotropic hypogonadism and deficiency in the TS levels. Further, total TS levels were significantly lower in the acute phase of severe TBI compared with mild and moderate TBI.[22] These observations suggest potential benefits of TS therapy after TBI in different aspects of neural cells physiology, including increased neuroenergetic efficiency coupled with a downregulation of apoptotic signals.

Here, a rodent model of severe TBI was used to explore effects of testosterone therapy after injury in context with mitochondria function.

Methods

Animals and treatment protocol

Ninety-day-old C57BL/6J male mice were obtained from Foundation for Health Science Research (FEPPS, Porto Alegre/RS, Brazil). A total of 30 animals (4–5 per cage) were placed into a controlled temperature room (22°C ± 1) under a 12 h light/12 h dark cycle (lights on at 7 A.M.) and had free access to food and water. The treatment consisted of a daily injection of an equal volume (50 μL) of corn oil (vehicle groups, VEH-SHAM, and VEH-controlled cortical impact (CCI); 10 animals per each group) or testosterone cypionate (15 mg/kg, based on previously published work[23]; Sigma-pharma, TS-CCI group; 10 animals per group), between 2 P.M. to 3 P.M for 10 days after the head trauma. Subsequently, animals were euthanized and the ipsilateral cortex surrounding the impact injury was dissected for neurochemical analysis. After CCI, animals were randomly assigned to both TS or VEH groups by two trained researchers. The treatment started 24 h after the CCI injury. The experimental design is outlined in Figure 1. All experiments were in agreement with the Committee on the Care and Use of Experimental Animal Resources, Universidade Federal do Rio Grande do Sul, Brazil, number 22436.

Controlled cortical impact (CCI) protocol

To cause TBI, mice were placed in the stereotaxic (Kopf Instruments, Tujunga, CA) with a heating bed (37 ± 1°C) and maintained with anesthesia inhalation (2.5% isoflurane) in a mixture of N_2 and O_2 (2:1) during the entire surgical procedure. A 4-mm diameter craniotomy was made in the central part of the left parietal bone to perform the CCI injury using an equipment Benchmark stereotaxic impactor (myNeuroLab; Leica, St. Louis, MO). The injury was induced by a piston of 3.0 mm diameter on the exposed surface of the intact dura mater. Other lesion parameters were fully adjusted in the equipment as follows: impact velocity of 5.7 m/sec; impact duration was 100 msec, and 2 mm of depth penetration. Soon after injury, the area of the craniotomy was isolated with a concave lamella bonded with dental cement, and the scalp was sutured. After the surgical procedure, anesthesia was discontinued and the animals were placed in a heated box to maintain normal body temperature and were monitored for 2 h post-injury.[24]

Modified Neurological Severity Score

The evaluation of CCI-induced neurological impairment was performed by two independent single-blinded trained researchers, 24 h after CCI injury using a modified Neurological Severity Score (mNSS). TS and vehicle administration were initiated after the mNSS test. The previously described 10-point scale[25] was modified to a 6-point scale, assessing functional neurological status of mice based on the presence of reflexes and the ability to perform motor and behavioral tasks, evaluated with the following behavioral composite: a) exit square; b) seeking behavior; c) straight walk; d) startle reflex; e) beam balancing; and f) round stick balancing. One point is awarded for failing to perform a task; thus, a normal, uninjured mouse scores 0.

Preparation of ipsilateral cortex homogenates

The whole ipsilateral cortex of mice were collected 10 days after CCI, and then homogenized in a specific buffer (320 mM sucrose, 1 mM EDTA, pH 7.4)[26] using a pre-cooled glass potter with 10 to 15 strokes. Following a centrifugation step of 1350 × g for 3 min at 4°C, the resulting mitochondria-enriched homogenates in the supernatant were aliquoted and used for respirometry, calcium handling, mitochondrial membrane potential, and hydrogen peroxide analysis. These assays were performed all simultaneously by the researchers according to their methodological skills in a time-frame of 10 min from euthanasia and start of the analysis, or sample processing for MTT assay. The samples were frozen at −80°C for protein quantification and further oxidative stress parameters and western blotting assays. The Pierce BCA Protein Assay Kit (Catalog #: 23225) was used for quantification of protein contents of the homogenized samples. The assay was performed according to the manufacturer's instructions. Measurements were performed in triplicates (coefficient of variation between duplicates was <3%) and corrected for the absorbance measured in the homogenization buffer only.

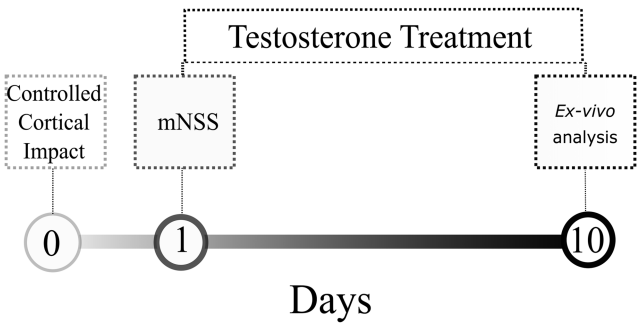

FIG. 1. Experimental design. Anesthetized mice were submitted to a single parasagittal severe controlled cortical impact (CCI) injury. Twenty-four hours later, they were submitted to modified Neurological Severity Score (mNSS) evaluation, and soon afterwards animals were injected with testosterone (TS) or vehicle (oil) for 10 days ($n = 10$, per group).

Mitochondrial calcium handling

To assess mitochondrial calcium buffering capacity, namely calcium influx and efflux, we measured the absorbance spectrophotometrically at 540 nm (Spectra Max M5; Molecular Devices). Mitochondria maintain the fluxes of ions across the inner membrane tightly controlled. This is particularly important because the dual physiological and detrimental roles of Ca^{2+} in the mitochondrial matrix.[11] Ipsilateral cortex homogenates (50 μL) obtained from 10-day-old treated mice were added to standard swelling incubation medium (100 mM KCl, 50 mM sucrose, 10 mM HEPES and 5 mM KH_2PO_4) and the basal mitochondrial absorbance was monitored during 3 min in microplates. Mitochondrial substrates PMGSA (3.5 mM pyruvate, 4.5 mM malate, 4.5 mM glutamate, 1.2 mM succinate and 100 μM of adenosine diphosphate [ADP]) were added to energize mitochondria and support ATP synthesis. Thus, the absorbance coupled with oxidative phosphorylation was monitored during 5 min. Afterward, calcium (Ca^{2+}, 20 mM) was added to induce large-amplitude swelling driven by the colloid osmotic force of Ca^{2+} influx at proteins localized in the mitochondrial matrix. The decrease in the absorbance caused by the Ca^{2+} influx was monitored for 10 min. After calcium-induced mitochondrial swelling, we accessed mitochondrial Ca^{2+} efflux as an indicator of shrinkage. Then, Na^+ (30 mM) was added to the medium and the increase in the absorbance was monitored for additional 10 min. For a mitochondrial-enriched suspension, the swelling and shrinkage causes a decrease and increase in the absorbance respectively, which are both discernible even to the naked eye.[27] Finally, we normalized all results for protein content. Also, we used the baseline Ca^{2+} from each group to standardize their own data, and calculated the percentage of variation in the absorbance (540 nm) after the addition of substrates (PMGSA) relative to basal; after addition of Ca^{2+} relative to PMGSA; and after addition of Na^+ relative to Ca^{2+}.

Mitochondrial membrane potential ($\Delta\Psi_m$)

The $\Delta\Psi_m$ was measured 10 days after CCI through the fluorescence signal emitted by the cationic dye safranin-O. Ipsilateral cortex homogenates were incubated in the respiration buffer used for the respirometry protocol, additionally supplemented with 10 μM safranin-O. The fluorescence was detected with an excitation wavelength of 495 nm and an emission wavelength of 586 nm (Spectra Max M5; Molecular Devices). An increased the fluorescence units mirror decreased $\Delta\Psi_m$ whereas decreased fluorescence units indicate increased $\Delta\Psi_m$. Baseline $\Delta\Psi_m$ was measured without addition of substrates and inhibitors in the incubation medium.

Further, pyruvate, malate, glutamate, succinate (PMGS) and ADP (2.5 mM) were incubated to modulate the activity of mitochondrial respiratory complex I, II, and V, and consequently $\Delta\Psi_m$. Increased ADP utilization after the addition of PMGS mirrors increased oxygen consumption coupled with ATP synthesis by the F0F1–ATP synthase (respiratory Complex V) along with decreased $\Delta\Psi_m$. Addition of the proton ionophore carbonyl cyanide 4-trifluoromethoxy-phenylhydrazone (FCCP 1 μM), a chemical uncoupler, triggers decrease in the $\Delta\Psi_m$ and oxidative phosphorylation while stimulating the maximal mitochondrial oxygen consumption. The addition of sodium azide (AZ; 20 mM), an inhibitor of mitochondrial respiratory complex IV (cytochrome oxidase), was used to decrease ATP synthesis and disrupt mitochondrial membrane potential. Moreover, we used the data achieved through the manipulation of mitochondrial respiratory rates with the components PMGS, ADP, FCCP, and AZ to calculate the percentage of change in the $\Delta\Psi_m$. Each component has a percentage of variation relative to the previous one. For instance, PMGS is relative to the baseline, and ADP is relative to the PMGS. Data are reported as arbitrary fluorescence units and were normalized to protein content.[28]

Mitochondrial respiratory protocol

The ipsilateral cortex of mice was dissected 10 days after CCI, then homogenized in a specific buffer (320 mM sucrose, 1 mM EDTA, 0.25 mM dithiothreitol, pH 7.4). Oxygen consumption measurements were performed using a standard respiration buffer (100 mM KCI, 75 mM mannitol, 25 mM sucrose, 5 mM phosphate, 0.05 mM EDTA, and 10 mM Tris-HC1; pH 7.4). Oxygen consumption per tissue mass was measured using the high-resolution Oxygraph-2k system and recorded real-time using DatLab software (Oroboros, Innsbruck, Austria). The results were normalized to the protein content. The experiments were performed at 37°C in a 2-mL chamber, with a modified multi-substrate titration protocol as previously described in detail elsewhere.[26]

Following 5 min for establishing routine respiration values, the multi-substrate titration protocol started. The protocol consisted of sequential addition of pyruvate, malate, and glutamate (PMG; 10, 10, and 20 mM, respectively) to obtain State IV (L) respiration; Subsequently, adenosine diphosphate (ADP, 2.5 mM) was titrated to obtain oxidative phosphorylation (OxPHOS) capacity of Complex I-Linked substrates (State III); maximal oxidative phosphorilation (OxPHOS) capacity (State III [P]) was obtained with the addition of succinate (S; 10 mM) in saturating ADP concentrations and non-mitochondrial respiration (ROX) after cyanide (KCN; 5 mM).

Respiratory fluxes were corrected automatically for instrumental background by DatLab taking into account oxygen consumption of the oxygen sensor and oxygen diffusion out of or into the oxygraph chamber measured at experimental conditions in incubation medium without biological sample. ROX was extracted from all of the above-mentioned states and tissue-mass specific oxygen fluxes were compared in different substrate and coupling states.

We calculated flux control factors (FCF), which express the change of flux in a single step of the SUIT protocol, normalized for the high flux as a specific reference state. The respiratory control ratio (RCR = State III [P]/State IV [L]) was obtained in the CI-linked substrate state. For statistical analysis RCR was transformed to its respective FCF, which is the OxPHOS coupling efficiency calculated as (P-L)/P = 1-L/P. The FCF for the CII-linked substrate stimulating STATE III respiration (succinate effect) was calculated as 1 – CI/CI&II, determined in the OxPHOS state in the protocol.[26–29] This analysis informs the influence of Complex II on the respirometry of other oxidative complexes. Since RCR ranges from 1.0 to infinity, we calculated the oxidative phosphorylation coupling efficiency, which has boundaries from 0.0 to 1.0 and is directly related to classic RCR (State III/State IV).

Mitochondrial H_2O_2 production and oxidative stress markers

The pattern of mitochondrial production of hydrogen peroxide (H_2O_2) under the modulation of TS was assessed in the ipsilateral cortex homogenates 10 days after CCI through the Amplex Red oxidation method. The same substrates, uncoupler, and inhibitors used in the respirometry protocol were incubated sequentially in the respiration buffer supplemented with 10 μM Amplex Red and 2 units/mL horseradish peroxidase to assess H_2O_2 generation. The baseline H_2O_2 level was measured without the presence of substrate in the incubation medium. Also, PMGS was used as the substrate to stimulate mitochondrial respiration, ADP to analyze the functional capacity of mitochondria to produce ATP, and the proton ionophore FCCP (Carbonyl cyanide 4-trifluoromethoxy-phenylhydrazone, a reversible inhibitor of mitochondrial oxidative phosphorylation) to estimate the maximal mitochondrial electron transport system capacity. Sodium azide was used to assess non-mitochondrial H_2O_2 production (ROX). Fluorescence was monitored at excitation (563 nm) and emission (587 nm) wavelengths with a Spectra Max M5 microplate reader (Molecular Devices).[28]

Moreover, at 10 days following CCI, we measured the activity of enzymes involved in the H_2O_2 production (superoxide dismutase [SOD]) and degradation (glutathione peroxidase [GPx]); the expression levels of the mitochondrial enzyme manganese superoxide dismutase (MnSOD) and total reactive oxygen species (ROS) production, altogether here designated as oxidative stress biomarkers. The measurements were performed, as described below.

2′7′-Dihydro-dichlorofluorescein (DCFH) oxidation assay

The measure of global ROS production in the ipsilateral cortex homogenates was performed using reduced 2′7′-dihydro-dichlorofluorescein diacetate (DCF-DA). Samples were incubated for 30 min at 37°C in the dark with 20 mM sodium phosphate, 140 mM KCl buffer pH 7.4 and 100 μM reduced 2′7′-Dichlorofluorescein diacetate (H_2DCF-DA) solution in a 96 wells plate. The H_2DCF-DA is enzymatically hydrolyzed by intracellular esterases and H_2DCF formed is oxidized by ROS being the DCF fluorescence (480 and 535 nm) proportional to the amount of ROS formed. The calibration curve was performed with standard DCF (0.25–10.0 μM), and the levels of reactive species were expressed as nmol of DCF formed per mg of protein.[30]

SOD activity assay

SOD activity in the ipsilateral cortex homogenates was determined based on the capacity of pyrogallol to autoxidize, a process highly dependent on superoxide radical.[31] The inhibition of autoxidation of this compound occurs in the presence of SOD, whose activity can be indirectly assayed spectrophotometrically at 420 nm. A calibration curve was performed with purified SOD as standard. A 50% inhibition of pyrogallol autoxidation is defined as one unit of SOD, and the specific activity was expressed as SOD units per mg of protein. The expression level of MnSOD was analyzed through Western blotting (see below).

GPx assay

GPx activity in the ipsilateral cortex homogenates was measured using tert-butylhydroperoxide as substrate.[32] The enzyme activity was determined by monitoring the nicotinamide adenosine dinucleotide phosphate (NADPH) disappearance at 340 nm. The medium contains 100 mM potassium phosphate, 1 mM ethylenediaminetetraacetic acid buffer pH 7.7, 0.4 mM azide, 2 mM glutathione reduced, 0.15 U/mL glutathione reductase, 0.1 mM NADPH, 0.5 mM tert-butyl-hydroperoxide, and supernatant sample. One GPx unit is defined as 1 μmol of NADPH consumed per minute. The specific activity was expressed as micromole of NADPH consumed per minute per mg of protein.

Western blotting

The ipsilateral cortex of mice was dissected 10 days after CCI and then homogenized in a buffer solution (EDTA 2 mM, protease and phosphatase inhibitor cocktails I and II; Sigma, St. Louis, MO) 0.001%, Tris HCl 50 mM, (pH 7,4), glycerol 10% and Triton X-100 1%) and centrifuged (1300 g/3 min). Supernatant was collected and diluted in an appropriated sample buffer. Samples of 20 μg of protein ($n = 6$–8 per group) were separated by electrophoresis on a 10% or 12% polyacrylamide gel and electrotransferred to PVDF (Amersham; GE Healthcare Life Sciences, Little Chalfont, UK) as previously reported.[33] Primary antibodies against Alpha-Spectrin (Millipore, GER; 1:1000; ref. MAB1622), calpain-2 (Cell Signalling; 1:1000; ref. 2539), anti-Bax (ABCAM; 1:1000; ref. ab7977), anti-BCL-2 (ABCAM; 1:1000; ref. ab7973); anti-MnSOD (ABCAM; 1:1000; ref. ab13533); anti-Tau phospho-S396 (ABCAM; 1:1000; ref. ab109390); anti-Tau antibody (ABCAM; 1:1000; ref. ab32057); caspase-3 (8G10; Cell Signalling; 1:1000; ref. 9665) cleaved caspase-3 (Cell Signalling; 1:1000; ref. 9664). All procedures were conducted according to specific antibody manufacturer's instruction. Primary antibodies were incubated overnight followed by 2 h incubation with horseradish peroxidase-conjugated anti-rabbit or anti-mouse IgG (1:5000; GE Healthcare Life Sciences) secondary antibodies. Membranes were incubated with Amersham ECL Western Blotting Detection Reagent (GE Healthcare Life Sciences) for 5 min and the immunodetection was made by chemoluminescence using Image Quant LAS 4000 (GE Healthcare Life Sciences). The protein expression was quantified using Image J software (Rockville, MD). The values of optic density were expressed as % of control.

Cell viability assay

Cell viability assay was performed 10 days after CCI through the colorimetric [3(4,5-dimethylthiazol-2- yl)- 2,5-diphenyl tetrazolium bromide] (MTT, Sigma) method.[34] Cell homogenates were incubated with 0.5 mg/mL of MTT, at 37°C during 45 min. The formazan product generated during the incubation was solubilized in dimethyl sulfoxide and measured at 560 and 630 nm. The results were expressed as the percentage of control.

Protein–protein interaction network and differential expression analysis

Functional interplay between proteins can often be inferred from genomic associations between the genes that encode them. The Search Tool for the Retrieval of Interacting Genes/Proteins (STRING) is a relational biological database and web source (https://string-db.org) used to store known and predicted protein–protein interactions. The database utilizes an interaction scoring system computed by combining the probabilities from different evidence channels and corrected for the probability of randomly observing and interaction. Input queries are associated using this scoring system and a graphical network representation can be generated to demonstrate their pairwise interactions. Network representations may provide insights of functional protein interactions (direct and indirect), which facilitate the analysis of modularity in biological processes.[35] The Protein–Protein Interaction (PPI) Network between the genes, Sdha and Sdhb (subunits of mitochondrial complex II-succinate dehydrogenase); Atp5d, Atp5a1 and Atp5c1 (subunits of mitochondrial complex V-ATP synthase), and SOD2; Bcl2 (B-Cell Lynphoma 2) and Bax (Bcl-2-like protein 4); Casp3 (caspase-3) and Capn2 (calpain-2); Mapt (microtubules associated protein Tau), was constructed using STRINGdb package (STRING version 10).[36] The network association topology obtained then was used to map transcriptomic analyses results with RedeR package.[37]

Based on the experimental molecular and functional results obtained, we searched gene expression data in TBI studies similar to ours (i.e., adult male mice strain C57BL/6) submitted to a single severe CCI injury in the dura matter, ipsilateral brain cortex samples analysis, and the end-point for the neurochemical analysis close to 10 days after the CCI. We found one study, which partially matched these criteria using adult male mice C57BL/6, submitted to severe CCI, and brain ipsilateral cortex gene expression profiling at Day 3 after CCI.[38] Expression data was obtained from Gene Expression Omnibus (GEO) using GEOquery package[39] under the identification GSE58485.[38] Using this dataset, differentially expressed genes of TBI versus control were obtained using the limma package.[40]

Statistical analysis

Results were calculated and expressed as the mean ± standard error of the mean. To analyze the differences between groups, we

used one-way analysis of variance followed by a *post hoc* Tukey test or Kruskal-Wallis test when necessary. All procedures were performed using GraphPad Prism 6.0 software. The differences were considered statistically significant at $p < 0.05$.

Results

Neurological score is impaired after CCI

As expected, we found higher neurological scores (mNSS) in the CCI group relative to SHAM implying in functional impairment of sensory-motor, spatial orientation, reflex, balance, and explorative behavior 24 h after the injury (data not shown).

Testosterone attenuated the calcium overload into mitochondria after CCI

Physiologically, there are small fluctuations in the intramitochondrial Ca^{2+} levels and even large transitory increments have low impact to cells integrity. While calcium is an essential signaling molecule, persistent high calcium levels result in overactivation of Ca^{2+}-dependent processes and mitochondrial calcium swelling. This mechanism has been considered the root for subsequent $\Delta\Psi_m$ depolarization, decreased ATP synthesis, and increased apoptotic signals observed in neurodegenerative disorders.[11] We found similar mitochondrial Ca^{2+} influx after the energization with PMGSA, implying that all groups were able to respond to a pulse of Ca^{2+} (Fig. 2A, 2B).

However, after the subsequent addition of Na^+ to the incubation medium in order to stimulate mitochondrial Ca^{2+} extrusion, the mitochondria swelling of VEH-CCI group remained elevated, indicating a persistent permanence of Ca^{2+} inside mitochondria. In contrast, VEH-SHAM and TS-CCI groups displayed an increase in absorbance, which illustrates a normal mitochondrial Ca^{2+} extrusion in the exchange with Na^+ (Fig. 2A, 2B). Taken together, these results indicate that CCI induced an increased mitochondrial Ca^{2+} swelling and deficient NCLX (Na^+-dependent) Ca^{2+} shrinkage. Remarkably, TS administration improved the Na^+-dependent control of Ca^{2+} levels within the mitochondria matrix in the TS-CCI group, implying it mediates NCLX function (Fig. 2A). Also, the percentage of variation in the Ca^{2+} swelling due to the addition of Na^+ was negative for CCI in relation to the other groups, which particularly that in spite of normal uptake, the Ca^{2+} ions did not transit b (Fig. 2B) back from the mitochondrial matrix to the cytosol.

Testosterone prevented the rupture of mitochondrial membrane potential ($\Delta\Psi_m$) dynamics after CCI

The entry of Ca^{2+} into the matrix brings together a positive charge, thereby generating a depolarizing current that partially dissipates the $\Delta\Psi_m$.[11] As mentioned, the $\Delta\Psi_m$ was measured through the fluorescence signal emitted by safranin-O after mitochondria from cortex homogenates had been energized and subsequently manipulated. The decrease in dye concentration in the medium parallels with the accumulation of the dye inside the mitochondria, which results in fluorescence quenching.[41] We showed that the $\Delta\Psi_m$ of VEH-CCI was significantly elevated at baseline and after the addition of FCCP compared with other groups. Also, the addition of the metabolic substrates (PMGS) increased the $\Delta\Psi_m$ in VEH-CCI relative to other groups while an inhibitor of ATP synthase complex (AZ) completely dissipates $\Delta\Psi_m$ in all groups. Remarkably, TS administration after CCI was able to rescue the $\Delta\Psi_m$ to levels of the control group at baseline, as well as after PMGS and FCCP. After the addition of ADP subsequent to PMGS, there was no apparent significant difference in the $\Delta\Psi_m$ between groups (Fig. 3A, 3B). However, it can be noticed that ADP was added subsequent to PMGS (meaning PMGS+ADP) then the comparison of $\Delta\Psi_m$ between PMGS vs. PMGS plus ADP shows that the VEH-CCI group does not respond to the stimulation whereas SHAM-VEH and TS-CCI groups had a decrease in the $\Delta\Psi_m$ of approximately 100%. Through the additional analysis of the percentage of variation, we confirmed the changes of $\Delta\Psi_m$ in the VEH-CCI group in response to ADP (Fig. 3B).

Moreover, the percentage of variation in the $\Delta\Psi_m$ between baseline and PMGS, PMGS and ADP, ADP and FCCP, and FCCP and AZ confirmed that independent of the mitochondrial target explored here, the VEH-CCI group did not effectively generate and dissipate $\Delta\Psi_m$ as did the TS-CCI and VEH-SHAM groups (Fig. 3B). These detectable alterations in the $\Delta\Psi_m$ may exert negative impact for the formation of proton gradient coupled with ATP synthesis (OxPHOS). Actually, when ADP was added to the incubation medium the VEH-CCI group displayed decreased OxPHOS capacity (Fig. 4C). Importantly, the percentage of variation in the Ψm between VEH-SHAM and TS-CCI groups was not significantly different, which highlights that TS-mediated effects on Ca^{2+} swelling also benefits $\Delta\Psi_m$.

Testosterone prevented the decrease in the OxPHOS coupling efficiency after CCI

It has long been recognized that $\Delta\psi$m is a critical parameter associated with the cellular capacity to generate ATP by oxidative phosphorylation. Indeed, the $\Delta\psi$m is the main component of the proton motive force generated beneath inner membrane during the electron transference through the mitochondrial respiratory complexes.[41] Given that neuroenergetics deficits are commonly associated with memory problems and neurodegeneration we additionally tested whether the alterations in the $\Delta\psi$m affect mitochondrial bioenergetics after CCI. Assessment of mitochondrial oxygen consumption was performed in the ipsilateral cortex homogenates. Different mitochondrial respiration states are shown in Figure 4. The representative standard SUIT protocol applied in the present study is illustrated by a VEH-SHAM sample (Fig. 4A). The oxygen consumption rate (OCR) level in the State III was significantly decreased in the VEH-CCI compared with the other groups (Fig. 4B). Also, mitochondrial succinate effect and OxPHOS coupling efficiency also was significantly impaired 10 days after CCI (Fig. 4C). Testosterone supplementation prevented the decrease in the OCR, OxPHOS Coupling efficiency, and the decrease in succinate effect (Fig. 4D). These functional alterations confirm that Ca^{2+} overload impairs $\Delta\psi$m and neuroenergetics efficiency, and suggests that brain oxygen consumption in response to metabolic substrates is partially diverted from ATP synthesis to production of ROS after CCI.

Testosterone attenuated mitochondrial hydrogen peroxide production following CCI

The mitochondrial oxidation of energy substrates coupled with electron transport system is considered the main site of ROS production including the H_2O_2. Here, the baseline H_2O_2 level 10 days after CCI was increased in the VEH-CCI compared with other groups (Fig, 5A). The addition of the mitochondrial substrates (PMGS and ADP), an uncoupler (FCCP), and a complex VI inhibitor (AZ) evoked a significant increase in the production of H_2O_2 by VEH-CCI and TS-CCI groups in relation to VEH-SHAM. However, TS administration after CCI (TS-CCI) caused a significant lower increment in the H_2O_2 level when compared with VEH-CCI, implying that

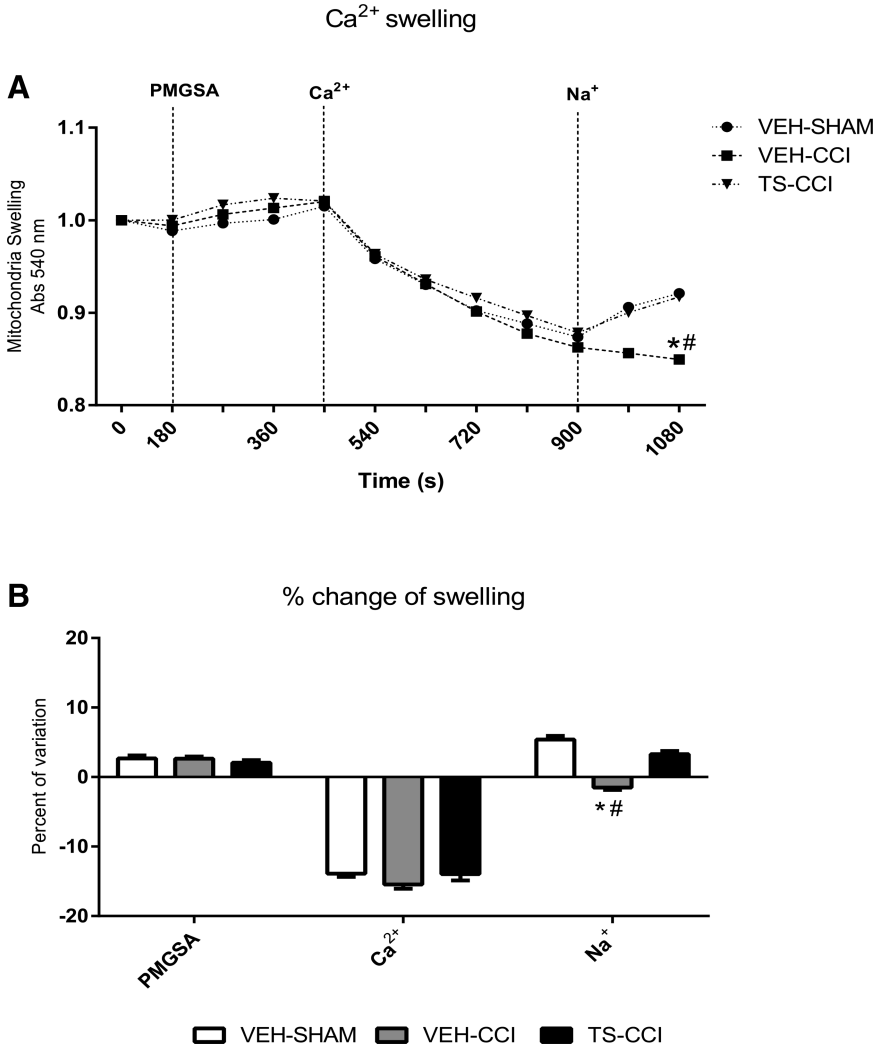

FIG. 2. Testosterone (TS) mediates mitochondrial calcium extrusion by the Na^+-dependent channel (NCLX) after controlled cortical impact (CCI). The mitochondrial Ca^{2+} swelling (that is, decrease absorbance at 540 nm) stimulated by the metabolic substrates pyruvate, malate, glutamate, succinate, and adenosine diphosphate (PMGSA) was similar between groups. Stimulation of Ca^{2+} extrusion (that is, increase absorbance at 540 nm) through the NCLX channel after addition of Na^+ was impaired in the vehicle (VEH)-CCI group (**A** and **B**). TS administration partially recovered the capacity of mitochondria to extrude Ca^{2+} from the matrix (A and B; $n = 6–8$, per group). *Significant difference compared with VEH-SHAM; #significant difference compared with TS-CCI.

testosterone attenuated mitochondrial mechanisms implicated in the rise of H_2O_2 levels (Fig. 5A, 5B). Likewise, TS decreased the total ROS levels in mice submitted to CCI, which replicates the regulatory role observed for H_2O_2 (Fig. 5B). No significant differences were found between groups concerning the enzymatic activity of SOD and GPx (Fig. 5C and Fig. 5D, respectively). However, the protein expression level of MnSOD decreased significantly in the VEH-CCI relative to VEH-SHAM group. Remarkably, 10 days of TS administration after CCI significantly heightened the expression of MnSOD (Fig. 5E), which highlights this protein as a molecular target of TS. Given that persistent increase in the H_2O_2 levels may cause cell damage, we further explored the mechanistic impact on biomarkers of apoptotic neurodegeneration.

Testosterone attenuated the expression of molecular biomarkers of neurodegeneration after CCI

The TBI induces a particular deformation in the neuronal morphology mirrored by axonal rupture and formation of varicosities.[10,42] Also, after TBI neurons displayed an abnormal aggregation of proteins, and increased phosphorylation and degradation of cytoskeletal proteins like Tau and alpha-Spectrin. These abnormalities are consistently associated with neurodegeneration. Here, we displayed increased immunocontent of $pTau^{Ser396}$/total Tau in VEH-CCI compared with VEH-SHAM and TS-CCI (Fig. 6A). Further, the Tau cleavage estimated by the ratio between total Tau (56 kDa)/Tau fragment (17 kDa) showed an increase in the Tau fragmentation after CCI (Fig. 6B). The expression levels of the calcium-activated proteolytic enzyme calpain-2 was significantly increased in VEH-CCI group compared with other groups (Fig. 6C). In addition, the axonal protein alpha-Spectrin (240 kDa), which is abnormally targeted by calpain-2 thereby generating cleaved products (150/145 kDa), was measured to estimate the neuronal damage (Fig. 6D). As expected, we found decreased alfa-Spectrin 240/150 ratio in the VEH-CCI group, compared with other groups implying increased protein degradation.

The relative increase in the protein Bax/BCL-2 ratio denotes the abundance of mitochondrial intrinsic apoptotic signals in VEH-CCI

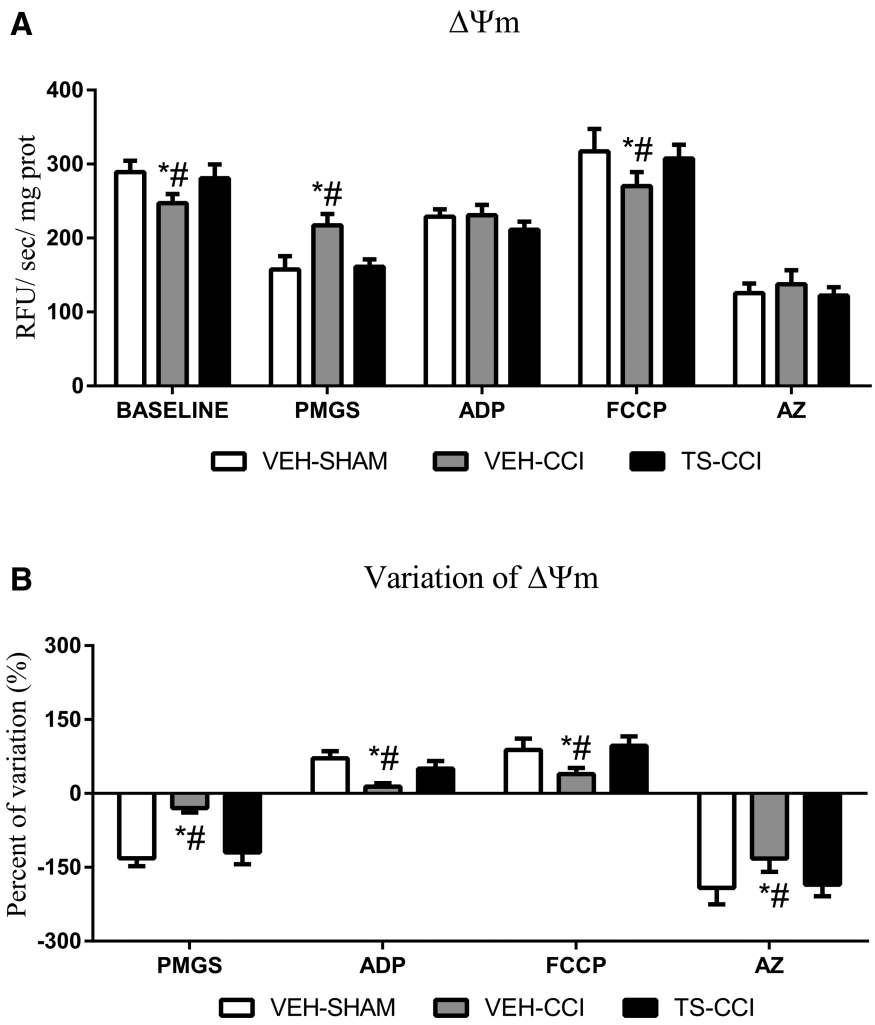

FIG. 3. Testosterone (TS) sustained the dynamics (generation and dissipation) of mitochondrial membrane potential ($\Delta\Psi_m$). **(A)** The fluorescent dye safranin-O is incorporated within the mitochondria of the ipsilateral cortex homogenates then decreasing the fluorescent signal of the medium. The $\Delta\Psi_m$ of the vehicle (VEH)-controlled cortical impact (CCI) was significantly different from VEH-SHAM and TS-CCI groups at baseline, after addition of the metabolic substrates pyruvate, malate, glutamate, and succinate (PMGS), and the uncoupler carbonyl cyanide 4-trifluoromethoxy-phenylhydrazone (FCCP). The percentage of variation **(B)** in the $\Delta\Psi_m$ between baseline and PMGS; PMGS and adenosine diphosphate (ADP); ADP and FCCP; and FCCP and AZ confirmed that the VEH-CCI group does not effectively generate and dissipate $\Delta\Psi_m$ as did TS-CCI and VEH-SHAM groups ($n = 6$–8, per group). *Significant difference compared with VEH-SHAM; #significant difference compared withf TS-CCI.

group (Fig. 6E). Moreover, an increased ratio of cleaved caspase-3/total caspase-3 reinforces the heightened proteolytic and apoptotic activities after CCI (Fig. 6F). As expected, there was significant decreased cell viability in VEH-CCI compared with VEH-SHAM and TS-CCI groups (Fig. 6G). Remarkably, 10 days of TS administration after CCI prevented the increase in the molecular effectors of neurodegeneration to date; Tau hyperphosphorylation and fragmentation, calpain-2 linked with alpha-Spectrin degradation, Bax/BCL-2 ratio, and cleaved caspase-3/total caspase-3. Therefore, the aforementioned preserved mitochondrial Ca^{2+} homeostasis and energy efficiency mediated by TS parallel with decreased apoptotic signals.

Protein–protein interactions

The resultant protein–protein interaction (PPI) network shows 11 genes/proteins in the nodes and association scores in the edges widths. The PPI network between the genes Sdha and Sdhb (subunits of mitochondrial complex II-succinate dehydrogenase), Atp5d, Atp5a1 and Atp5c1 (subunits of mitochondrial complex V-ATP synthase), SOD2 (manganese superoxide dismutase-2), Bcl2 and Bax; Casp3 (caspase-3) and Capn2 (calpain-2); Mapt (microtubules associated protein Tau) highlights two distinct clusters denoting CCI-induced signature: The right side cluster contains genes linked with mitochondrial bioenergetics and the left side cluster contains genes related to apoptotic neurodegeneration. After investigating the expression profile of these genes using the GSE58485 study, we can observe that the mitochondrial bioenergetics cluster is downregulated in CCI (lighter grey), whereas the apoptosis cluster is upregulated in CCI (black) compared with the control group. Also, the two clusters interact functionally through mitochondrial superoxide dismutase (SOD2) gene, thus they are influencing each other in terms of cell physiology (Fig. 7).

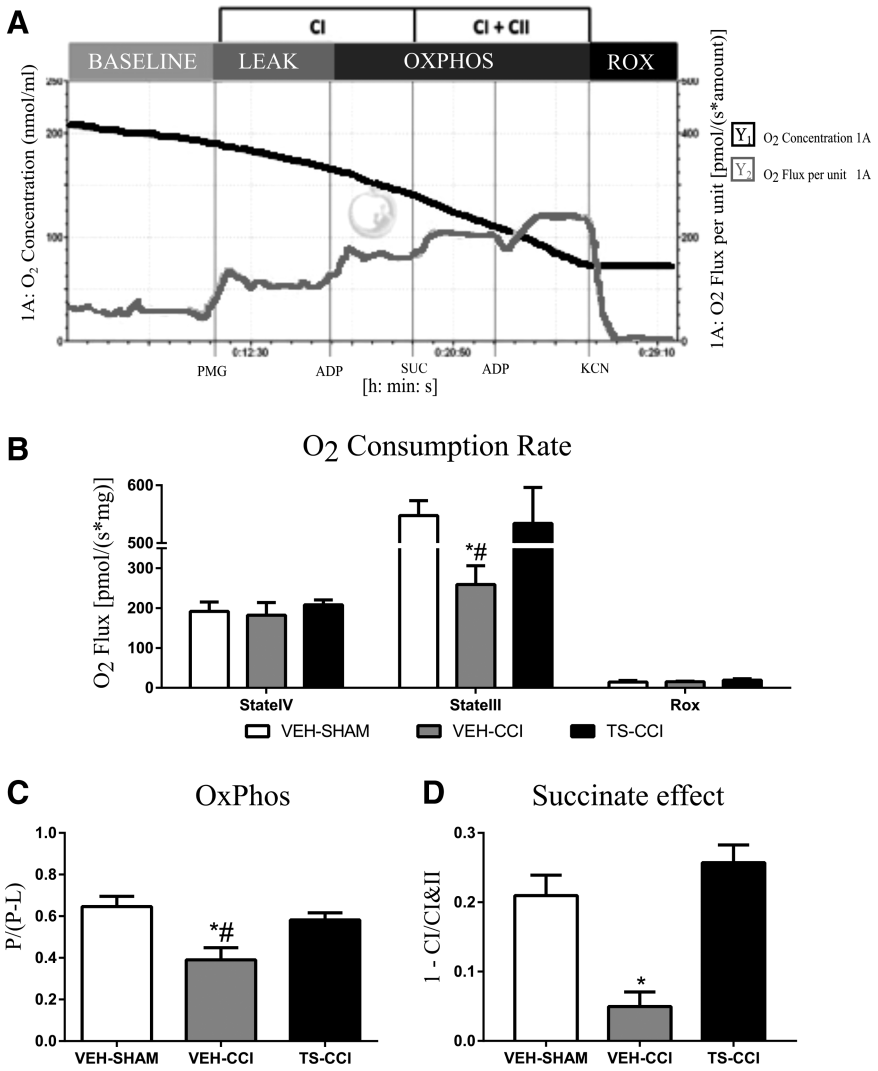

FIG. 4. Oxygen consumption in different mitochondrial states 10 days after controlled cortical impact (CCI). The representative standard SUIT protocol of vehicle (VEH)-SHAM mice illustrates the profile of oxygen consumption by an ipsilateral cortex homogenate after the addition of pyruvate, malate, and glutamate (PMG), adenosine diphosphate (ADP), succinate (Suc), carbonyl cyanide 4-trifluoromethoxy-phenylhydrazone (FCCP), and cyanide (KCN) **(A)**; oxygen consumption rate at different mitochondrial states **(B)**; oxidative phosphorylation (OxPHOS) coupling efficiency **(C)** and succinate effect **(D)** were significantly decreased after CCI. Testosterone (TS) administration attenuated the mitochondrial bioenergetics dysfunction after CCI (B, C, and D; $n = 6–8$, per group). *Significant difference compared with VEH-SHAM; #significant difference compared with TS-CCI.

Discussion

In the present study, TS administration after TBI was found to preserve crucial mitochondrial function linked with energy production. Efficacious effects included, maintaining Ca^{2+} homeostasis, membrane potential, the influence of succinate on global oxidative complexes respirometry, and OxPHOS coupling. Collectively, these actions prevented alterations associated with neurodegeneration. These results suggest that TS treatment maintained aspects of mitochondrial function that promote ATP synthesis, thereby maintaining cell survival after severe injury.

It has been well established that pituitary and gonadal hormone levels are often decreased in the brain and plasma after a TBI. This occurs across the acute setting and persists in long-term survival, typically in association with neurological dysfunction.[19–22] Accordingly, TS supplementation after severe TBI appears to be an attractive strategy to reverse persisting neurogenetic deficiencies and reduce neurodegeneration, albeit there are few studies addressing pharmacokinetics and pharmacodynamics characteristics of this drug after TBI, which could provide a better background for dose choices and time regimens.[7,8,43,44]

In a normal cell environment, a transitory increase in the Ca^{2+} levels within mitochondrial matrix is a key activator of ATP synthesis and other Ca^{2+} sensitive processes, whereas a persistent Ca^{2+} elevation can disturb ATP synthesis and promote apoptotic signaling.[7–9] Interestingly, reports have shown that in the acute phase after TBI, brain mitochondria import Na^{+} and Ca^{2+} via NCLX in a putative reverse mode, which then contributes with increased neuronal death.[45–47] The current data provide the first evidence that TS treatment addresses this pathological NCLX function after TBI, although the downstream effect on ATP synthesis was not elucidated.[47] While it is not well established if mitochondrial swelling is

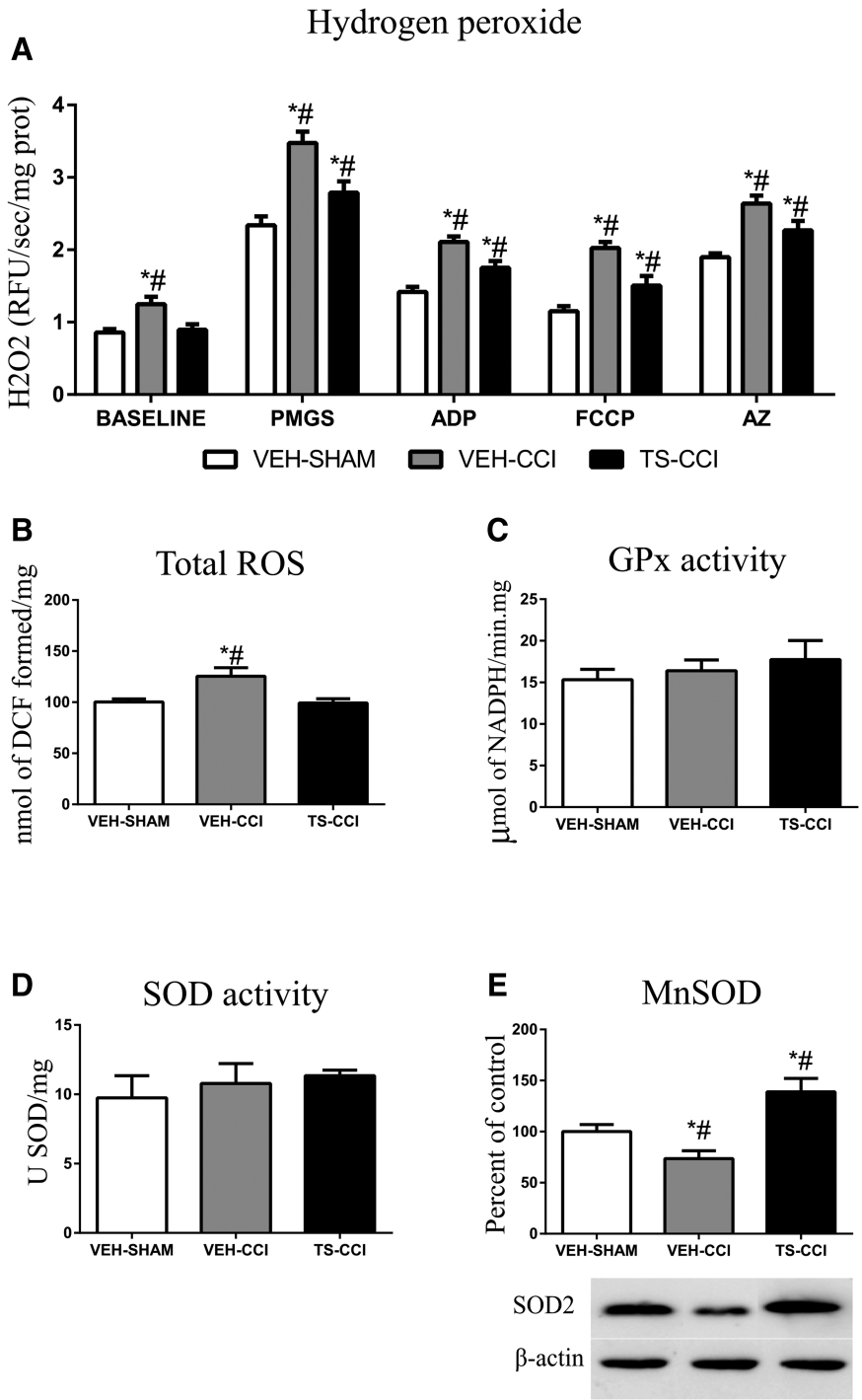

FIG. 5. Mitochondrial hydrogen peroxide (H_2O_2) production and oxidative stress parameters after controlled cortical impact (CCI). The H_2O_2 levels in the ipsilateral cortex at baseline and after the addition of substrates (pyruvate, malate, glutamate, and succinate [PMGS] and adenosine diphosphate [ADP]), uncoupler carbonyl cyanide 4-trifluoromethoxy-phenylhydrazone (FCCP) and ATP synthase inhibitor (AZ) are shown after CCI. **(A).** Testosterone administration for 10 days after CCI significantly decreased the H_2O_2 levels after CCI ($n = 6$–8, per group). *Significant difference compared with vehicle (VEH)-SHAM; #significant difference when compared with TS-CCI.

a strictly inner-membrane phenomenon, it should be taken into consideration that Ca^{2+}-induced mitochondrial swelling and subsequent cell death require an increase in the Ca^{2+} influx or alternatively, a decrease in the inner membrane calcium efflux.[48] Given that Ca^{2+} mediates a variety of neurotoxic secondary events after TBI, the current study addressed potential mechanisms.[46–48] In particular, it was found that TBI impaired Na^{+}-stimulated Ca^{2+} efflux through the NCLX, which appears to account for persisting increases in Ca^{2+} concentrations inside the mitochondria. Notably, in the injured mice receiving TS treatment, the NCLX was

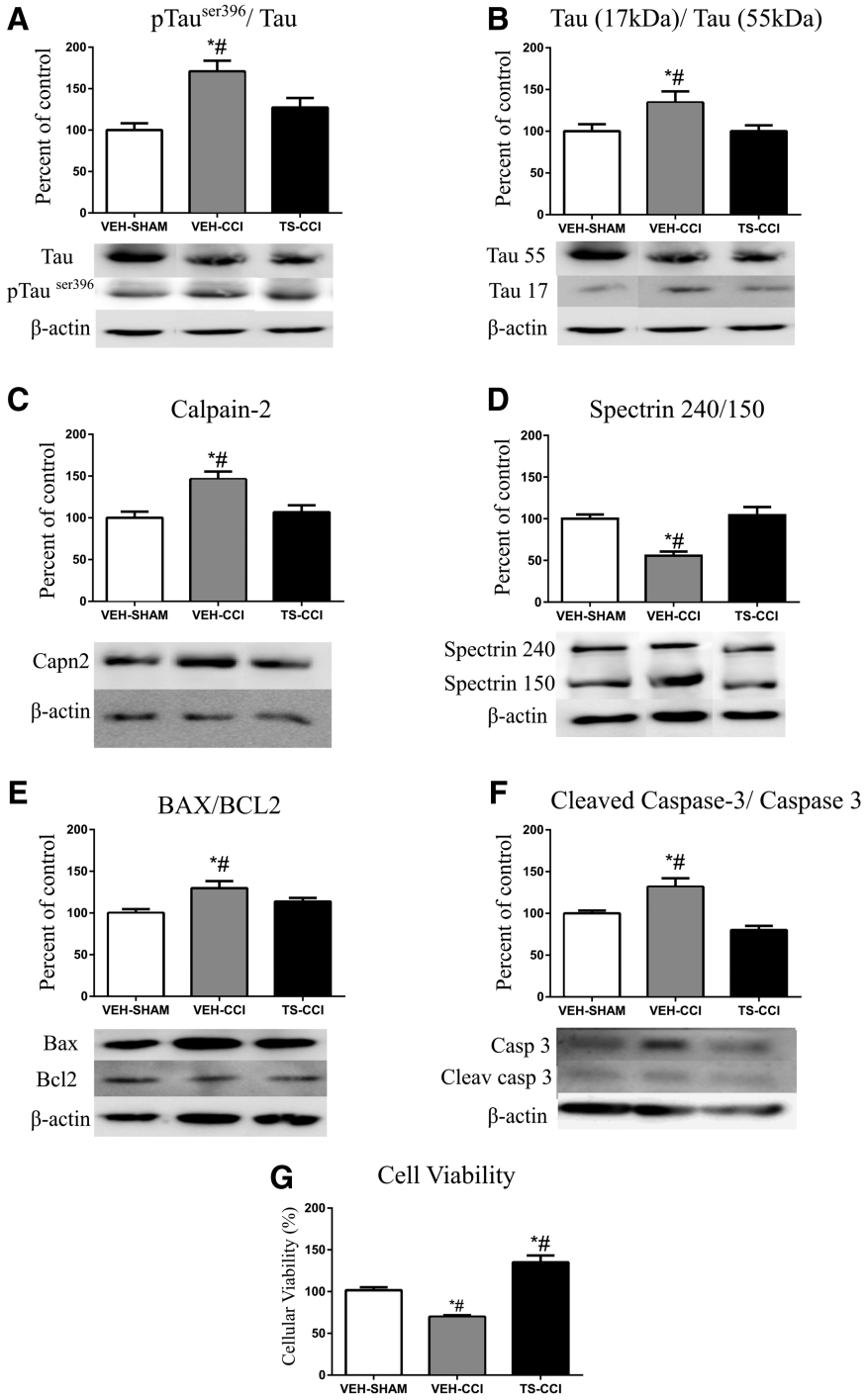

FIG. 6. Testosterone (TS) attenuates molecular effectors of neurodegeneration after a severe controlled cortical impact (CCI). A CCI event significantly altered the protein expression levels of Tau phosphorylated at Ser396 **(A)** and stimulated Tau protein fragmentation **(B).** Further, increase in the immunocontent of calpain-2 **(C)** and fragmentation of its substrate alfa-spectrin **(D)** suggests an exacerbated calcium-activated protease activity. The expression of apoptotic effectors Bax/Bcl2 **(E)** and cleaved caspase-3 **(F)** were increased in the ipsilateral cortex after CCI, followed by decreased cell viability **(G).** Testosterone administration attenuated the expression levels of the mentioned effectors of neurodegeneration (A, B, C, D, and F; $n = 6$, per group). *Significant difference compared with VEH-SHAM. #Significant difference compared with TS-CCI.

responsive to Na^+ and extruded Ca^{2+}, which potentially contributed to preserving the mitochondrial energy efficiency.

Changes in oxidative metabolism like the $\Delta\psi m$, and activity of ETS complexes behave in response to Ca^{2+} also appeared to play an important role in post-TBI pathophysiology. Ca^{2+} influx results in a net positive charge in the matrix, leading to alterations in the net charge across the mitochondrial internal membrane and a change in $\Delta\psi m$ depolarization. However, there remains debate regarding if or how the NCLX exerts influence on $\Delta\psi m$.45 In particular, it has been challenging to determine potential contribution of other

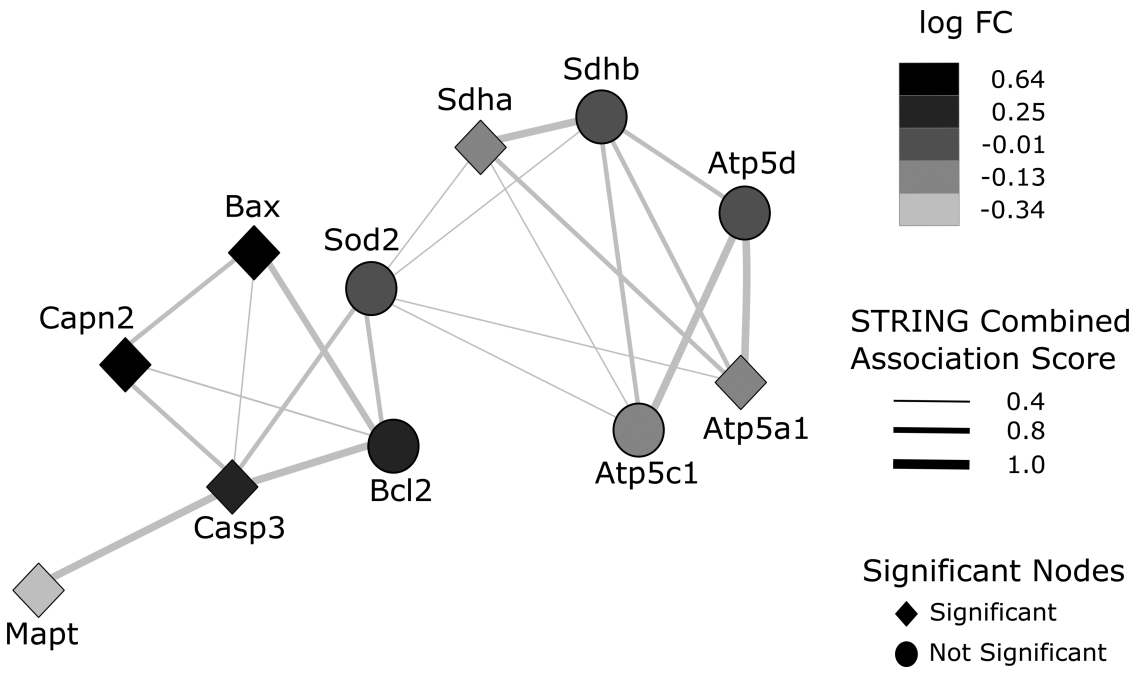

FIG. 7. Protein–Protein interaction (PPI) network representation of differential expression analysis. GEO dataset GSE58485 was used to compare controlled cortical impact (CCI) versus control samples, and STRING was employed to obtain known associations between 11 genes/proteins of interest showed in the nodes and association scores in the edges widths. The results from the differential expression analysis of these genes were mapped over the PPI network topology. PPI network between the genes Sdha and Sdhb (subunits of mitochondrial complex II-succinate dehydrogenase), Atp5d, Atp5a1, and Atp5c1 (subunits of mitochondrial complex V-ATP synthase), SOD2 (manganese superoxide dismutase-2), Bcl2 and Bax; Casp3 (caspase-3) and Capn2 (calpain-2); Mapt (microtubules associated protein Tau) highlight two distinct clusters: The right side cluster contains genes linked with mitochondrial bioenergetics and the left side cluster contains genes related to apoptotic neurodegeneration. After investigating the expression profile of these genes using GSE58485 study, we observed that the mitochondrial bioenergetics cluster is downregulated in CCI (lighter gray), whereas the apoptosis cluster is upregulated in CCI (black)m compared with the control. Also, the two clusters interact functionally through mitochondrial superoxide dismutase (SOD2) gene, thus they are influencing each other in terms of cell physiology.

mitochondrial ionic transporters that can also influence the Na^+ and Ca^{2+} gradients.[49]

In normal respiring mitochondria, the $\Delta\Psi m$ is primarily achieved by pumping protons from the matrix to intermembrane space through some ETS complexes. This is synchronized with the proton motive force driven ATP synthesis by the F0F1-ATP synthase. Given the functional proximity between electrochemical properties of the mitochondrial internal membrane and ATP synthesis, the present study examined the effect of challenging mitochondria in a respiratory protocol. Based on this approach, functional aspects of oxidative phosphorylation, such as substrate uptake and oxidation, F0F1-ATP synthase activity, ubiquinone and cytochrome C pool size, and specific electron transport complexes activities can be evaluated using the RCR (respiratory control ratio), which is a respiratory index of the degree of metabolic coupling between ETS and oxidative phosphorylation.[26–29]

Recently, Hill and colleagues[50] showed that isolated mitochondria from the ipsilateral cortex 3 days after TBI, present a deficient metabolism, which was followed by a recovery at Day 5 after injury. The authors hypothesized that by 5 days post-injury, no dysfunctional mitochondria remain in the injured brain.[50] In contrast to the present study, a previous report demonstrated responses of mitochondria to treatments with substrates and inhibitors after TBI appeared to be dependent on the localization of mitochondria at synaptic and non-synaptic sites.[51] The different findings may reflect the use of homogenates from ipsilateral cortex enriched in mitochondria for the respirometry protocol in the present study. The results identify prolonged dysfunctions in the Complex V (F0F1-ATP synthase) 10 days after TBI. As global metabolic consequences, the OCR by mitochondria in the State III is not efficiently coupled with ATP synthesis (OxPHOS), implying that at least in part, the oxygen consumption is not appropriately coupled with ATP production. In contrast with these findings, other recent studies have shown significant differences in the State IV between Sham and CCI groups up to 5 days after CCI likely due differences related to the gradient preparation and tissue collection.[50,51]

An uncontrolled mitochondrial metabolic uncoupling is a key mechanism leading to ROS production in brain pathologies, including TBI.[8–12,51] When mitochondria dysfunction persists, the mitochondria themselves begin to consume ATP, burn energy of nutrients as heat, swell upon Ca^{2+} overload. This leads to production of deleterious compounds, such as ROS that directly attack and damage mitochondria as well as other cellular structures.[12,50–52] The present results demonstrate that after severe TBI, mitochondrial H_2O_2 production remained elevated across the entire respiratory protocol, and that TS supplementation attenuated the H_2O_2 overproduction. Similarly, TS supplementation attenuated total ROS (superoxide anion, hydroxyl radicals, lipid hydroperoxides, and H_2O_2 levels), confirming that increased H_2O_2 quantitatively impacts the global pro-oxidative status. Demonstrations that high ROS levels induce oxidative damage to the components of neural cell membranes and mitochondria have often been seen in TBI studies, and together with Ca^{2+} overload, may represent to mitochondrial dysfunction as a deleterious feed-forward cycle.[12,52] This

is supported by the study by Hill and colleagues,[50] which demonstrated that the time course of the mitochondrial respiratory alterations in the cortex and hippocampus after CCI in the rat, runs in parallel with the evolution of oxidative damage to mitochondria and cellular proteins.

The current data also demonstrate that in addition to decreased Succinate levels and ATP synthesis induced by TBI, the elevation of H_2O_2 represents a direct manifestation of prolonged mitochondrial dysfunction, which apparently has the Ca^{2+} overload as the main trigger. As an antidote of oxidative damage, endogenous ROS-detoxifying systems (enzymatic and non-enzymatic) in mitochondria remove excessive ROS. In the present study, total SOD and GPx activities were found to be not affected by TS treatment post-injury despite elevated total ROS and H_2O_2.

At the protein level, mitochondrial MnSOD immunocontent was decreased after injury in the present study but overexpressed in the TS-CCI group, indicating transcriptional and/or post-translational influences. Remarkably, mitochondrial-associated oxidative stress can initiate stimulation or induction of the antioxidant gene SOD2, whose protein has enhancing cell survival properties. In the present study, it was found that the MnSOD immunocontent and H_2O_2 levels displayed opposite profiles. This is somewhat unexpected because the enzyme converts superoxide anion to H_2O_2, in turn, which is neutralized mainly by the GPx activity. Likewise, in a previous study, CCI study in mice showed that even in the presence of increased lipid peroxidation (by 4-hydroxynonenal) the gene expression of CuSOD (cytosolic) and MnSOD (mitochondrial) in the cortex and hippocampus did not vary over the course of 1 week, although the transcription factor of antioxidant response elements (Nrf2-ARE) was overexpressed.[53] Therefore, the long-term increase in H_2O_2 levels observed after TBI in the present study appear to be most related to the effects of persistently increased Ca^{2+} levels on mitochondria metabolism, or alternatively by the electron reductive force direct on superoxide anion, rather than by SOD expression.[54]

A particular structural aspect of TBI that is associated with progressive neurodegeneration is the axonal pathology leading to the destabilization of microtubules associated proteins, axonal accumulation of neurotoxic proteins, and degradation of neuronal cytoskeletal proteins mainly by Ca^{2+}-dependent proteases.[10,42] For instance, hyperphosphorylated Tau protein aggregates within neurites and neuronal cell bodies are present after TBI, the degree of which correlates with progressive neuronal dysfunction, functional decline, and behavioral changes, observed in both in humans and rodents.[3,42,55]

Elevated cytosolic Ca^{2+} after TBI increase the activity of protein kinases involved in the aberrant phosphorylation of Tau, as well as trigger the proteolysis of the cytoskeletal protein alpha-Spectrin by calpain-2. Also, excessive intramitochondrial Ca^{2+} concentrations stimulate permeability transition pore formation and cytochrome C release, which in turn raises caspase-3 proteolytic activity.[12] Although both calpain-2 and caspase-3 are able to cleave alpha-Spectrin in 150 kDa fragments, it has been demonstrated that at a short time-window after TBI the breakdown by calpain-2 overcomes caspase-3.[56,57]

In the present study, it was found that TS treatment post-TBI prevented the overexpression of $pTau^{Ser396}$, calpain-2 and cleaved caspase-3 ratio after CCI. This was accompanied by decreased Tau fragmentation (55/17 kDa) and alpha-Spectrin fragmentation (150 kDa). In both humans and rodents, the levels of alpha-Spectrin in serum and brain tissue have been found to increase after TBI and remain elevated from 12 h to 6 days before decreasing to basal levels.[56–58] Intriguingly, in a rodent TBI model of axonal injury, prolonged calpain activation (4 to 14 days) correlated with subsequent cell death.[59] Accordingly, TS administered for 10 days post-TBI in the present study appears to have protected neurons that would have otherwise degenerated due to secondary pathological cascades.

Further, the activation of caspase-3 by cleavage also culminates in degradation of cytoskeletal proteins, and together with energy impairment and exacerbated ROS production, it has been linked with mitochondrial dysfunction and apoptosis. Here, a predominance of the expression of pro-apoptotic protein Bax relative to anti-apoptotic protein Bcl-2 was observed after TBI, which was attenuated by TS treatment. The resulting increase in cell viability in the TS-treated animals suggests an increase of mitochondrial survival helped prevent apoptosis.[60]

This study also allowed for the development of an association network to examine the effect of severe TBI in the mouse on the expression of various genes and proteins using the STRING database.[61] Therefore, we acquired a high-throughput transcriptional dataset (GSE58485) with similar methodological characteristics to our CCI protocol and evaluated differential expression patterns of key molecular players driving the secondary pathology. From the relatively small STRING interaction query used in the present study, two distinct clusters were observed, illustrating a mechanistic integration between mitochondrial bioenergetics failure and increments of apoptotic signaling. Within the bioenergetics cluster, the subunits of ATP synthase, succinate dehydrogenase, and SOD2 are highly connected. Remarkably, SOD2 is an important regulator of superoxide levels originated from the oxidative metabolism, thus the association with mitochondria cluster could be expected, reassuring the biological validity of this network. Also, SOD2 serve as the bridge between the two clusters and is highly connected with Casp3 and Bcl2, genes associated with apoptotic neurodegeneration.

Overall, it was found that short-term TS supplementation after a severe TBI preserved normal mitochondrial Ca^{2+} management and energy efficiency, thereby, preventing cell death via apoptosis. In particular, modulation of mitochondrial NCLX activity by TS was found to play a central role in this cell preservation. Accordingly, the current data highlights the importance of maintaining normal TS levels after TBI, which appears to specifically address post-injury mitochondria dysfunction.

Acknowledgments

The authors would like to thank the Center for Brain Injury and Repair, University of Pennsylvania (CBIR-UPENN) for the technical and scientific support, the Brazilian scientific agencies/programs INNT-CNPq #465346, CNPq # 401645/2012-6, CAPES, FAPERGS-Pronex, FAPERGS-PPSUS # 03/2017, and support from the US National Institute of Neurological Disorders and Stroke of the National Institutes of Health under award numbers R01NS092398, R01NS094003, and R01NS038104.

Author Disclosure Statement

No competing financial interests exist.

References

1. Meaney, D.F., Morrison, B., and Dale Bass, C. (2014). The mechanics of traumatic brain injury: a review of what we know and what we need

to know for reducing its societal burden. J. Biomech. Eng. 136, 021008.
2. Rosenfeld, J.V., Maas, A.I., Bragge, P., Morganti-Kossmann, M.C., Manley, G.T., and Gruen, R.L. (2012). Early management of severe traumatic brain injury. Lancet 380, 1088–1098
3. Blennow, K., Hardy, J., and Zetterberg, H. (2012). The neuropathology and neurobiology of traumatic brain injury. Neuron 76, 886–899.
4. Johnson, V.E., Weber, M.T., Xiao, R., Cullen, D.K., Meaney, D.F., Stewart, W., and Smith, D.H. (2018). Mechanical disruption of the blood–brain barrier following experimental concussion. Acta Neuropathol. 135, 711–726.
5. Meng, Q., Zhuang, Y., Ying, Z., Agrawal, R., Yang, X., and Gomez-Pinilla, F. (2017). Traumatic brain injury induces genome-wide transcriptomic, methylomic, and network perturbations in brain and blood predicting neurological disorders. EBioMedicine 16, 184–194.
6. Gilmer, L.K., Roberts, K.N., Joy, K., Sullivan, P.G., and Scheff, S.W. (2009). Early mitochondrial dysfunction after cortical contusion injury. J. Neurotrauma 26, 1271–1280.
7. Hiebert, J.B., Shen, Q., Thimmesch, A.R., and Pierce, J.D. (2015). Traumatic brain injury and mitochondrial dysfunction. Am. J. Med. Sci. 350, 132–138.
8. Pandya, J.D., Nukala, V.N., and Sullivan, P.G. (2013). Concentration dependent effect of calcium on brain mitochondrial bioenergetics and oxidative stress parameters. Front. Neuroenergetics 5,10.
9. Vekaria, H.J., Talley Watts, L., Lin, A.L., and Sullivan, P.G. (2019). Targeting mitochondrial dysfunction in CNS injury using methylene blue; still a magic bullet? Neurochem. Int. 109, 117–125.
10. Johnson, V.E., Stewart, W., Weber, M.T., Cullen, D.K., Siman, R., and Smith, D.H. (2016) SNTF immunostaining reveals previously undetected axonal pathology in traumatic brain injury. Acta Neuropathol. 31, 115–135.
11. Jafri, M.S. and Kumar, R. (2014). Modeling mitochondrial function and its role in disease. Prog. Mol. Biol. Transl. Sci. 123, 103–125.
12. Ji, J., Tyurina, Y.Y., Tang, M., Feng, W., Stolz, D.B., Clark, R.S., Meaney, D.F., Kochanek, P.M., Kagan, V.E., and Bayır, H. (2012). Mitochondrial injury after mechanical stretch of cortical neurons in vitro: biomarkers of apoptosis and selective peroxidation of anionic phospholipids. J. Neurotrauma 29, 776–788.
13. Gajavelli, S., Sinha, V.K., Mazzeo, A.T., Spurlock, M.S., Lee, S.W., Ahmed, A.I., Yokobori, S., and Bullock, R.M. (2015). Evidence to support mitochondrial neuroprotection, in severe traumatic brain injury. J. Bioenerg. Biomembr. 47, 133–148.
14. Cheng, G., Kong, R.H., Zhang, L.M., and Zhang, J.N. (2012). Mitochondria in traumatic brain injury and mitochondrial-targeted multipotential therapeutic strategies. Br. J. Pharmacol. 167, 699–719.
15. Hatanaka, Y., Hojo, Y., Mukai, H., Murakami, G., Komatsuzaki, Y., Kim, J., Ikeda, M., Hiragushi, A., Kimoto, T., and Kawato, S. (2015). Rapid increase of spines by dihydrotestosterone and testosterone in hippocampal neurons: dependence on synaptic androgen receptor and kinase networks. Brain Res. 1621, 121–132.
16. Fanaei, H., Karimian, S.M., Sadeghipour, H.R., Hassanzade, G., Kasaeian, A., Attari, F., Khayat, S., Ramezani, V., and Javadimehr, M. (2014). Testosterone enhances functional recovery after stroke through promotion of antioxidant defenses, BDNF levels and neurogenesis in male rats. Brain Res. 1558, 74–83.
17. Gurer, B., Kertmen, H., Kasim, E., Yilmaz, E.R., Kanat, B.H., Sargon, M.F., Arikok, A.T., Ergüder, B.I., and Sekerci, Z. (2015). Neuroprotective effects of testosterone on ischemia/reperfusion injury of the rabbit spinal cord. Injury 46, 240–248.
18. Hioki, T., Suzuki, S., Morimoto, M., Masaki, T., Tozawa, R., Morita, S., and Horiguchi, T. (2014). Brain testosterone deficiency leads to down-regulation of mitochondrial gene expression in rat hippocampus accompanied by a decline in peroxisome proliferator-activated receptor-gamma coactivator 1alpha expression. J. Mol. Neurosci. 52, 531–537.
19. Lopez-Rodriguez, A.B., Acaz-Fonseca, E., Spezzano, R., Giatti, S., Caruso, D., Viveros, M.P., Melcangi, R.C., and Garcia-Segura, L.M. (2016). Profiling neuroactive steroid levels after traumatic brain injury in male mice. Endocrinology 157, 3983–3993.
20. Bavisetty, S., Bavisetty, S., McArthur, D.L., Dusick, J.R., Wang, C., Cohan, P., Boscardin, W.J., Swerdloff, R., Levin, H., Chang, D.J., Muizelaar, J.P., and Kelly, D.F. (2008). Chronic hypopituitarism after traumatic brain injury: risk assessment and relationship to outcome. Neurosurgery 62, 1080–1093.
21. Tanriverdi F, Senyurek H, Unluhizarci K, Selcuklu A, Casanueva FF, and Kelestimur F. (2006). High risk of hypopituitarism after traumatic brain injury: a prospective investigation of anterior pituitary function in the acute phase and 12 months after trauma. J. Clin. Endocrinol. Metab. 91, 2105–2111.
22. Tölli, A., Borg, J., Bellander, B.M., Johansson, F., and Höybye, C. (2017). Pituitary function within the first year after traumatic brain injury or subarachnoid haemorrhage. J. Endocrinol. Invest. 40, 193–205.
23. Martinez-Sanchis, S., Salvador, A., Moya-Albiol, L., Gonzalez-Bono, E., and Simon, V.M. (1998). Effects of chronic treatment with testosterone propionate on aggression and hormonal levels in intact male mice. Psychoneuroendocrinology 23, 275–293.
24. Smith, D.H., Soares, H.D., Pierce, J.S., Perlman, K.G., Saatman, K.E., Meaney, D.F., Dixon, C.E., and McIntosh, T.K. (1995). A model of parasagittal controlled cortical impact in the mouse: cognitive and histopathologic effects. J. Neurotrauma 12, 169–178.
25. Albert-Weissenberger, C., Varrallyay, C., Raslan, F., Kleinschnitz, C., and Siren, A.L. (2012). An experimental protocol for mimicking pathomechanisms of traumatic brain injury in mice. Exp. Transl. Stroke Med. 4, 1.
26. Gnaiger, E. (2014). *Mitochondrial Pathways and Respiratory Control. An Introduction to OXPHOS Analysis,* 4th ed. OROBOROS MiPNet Publications: Innsbruck, Austria.
27. Luongo, T.S., Lambert, J.P., Gross, P., Nwokedi, M., Lombardi, A.A., Shanmughapriya, S., Carpenter, A.C., Kolmetzky, D., Gao, E., van Berlo, J.H., Tsai, E.J., Molkentin, J.D., Chen, X., Madesh, M., Houser, S.R., and Elrod, J.W. (2017). The mitochondrial Na(+)/Ca(2+) exchanger is essential for Ca(2+) homeostasis and viability. Nature 545, 93–97.
28. Portela, L.V., Brochier, A.W., Haas, C.B., de Carvalho, A.K., Gnoato, J.A., Zimmer, E.R., Kalinine, E., Pellerin, L., and Muller, A.. (2017). Hyperpalatable diet and physical exercise modulate the expression of the glial monocarboxylate transporters MCT1 and 4. Mol. Neurobiol. 54, 5807–5814.
29. Burtscher, J., Zangrandi, L., Schwarzer, C., and Gnaiger, E. (2015). Differences in mitochondrial function in homogenated samples from healthy and epileptic specific brain tissues revealed by high-resolution respirometry. Mitochondrion 25, 104–112.
30. LeBel, C.P., Ischiropoulos, H., and Bondy, S.C. (1992). Evaluation of the probe 2′,7′-dichlorofluorescin as an indicator of reactive oxygen species formation and oxidative stress. Chem. Res. Toxicol. 5, 227–231.
31. Marklund, S. (1985). *Pyrogallol Autoxidation.* CRC Press, Inc.: Boca Raton, FL.
32. Wendel A. (1981). Glutathione peroxidase. Methods Enzymol. 77, 325–333.
33. Muller, A.P., Gnoatto, J., Moreira, J.D., Zimmer, E.R., Haas, C.B., Lulhier, F., Perry, M.L., Souza, D.O., Torres-Aleman, I., and Portela, L.V. (2011). Exercise increases insulin signaling in the hippocampus: physiological effects and pharmacological impact of intracerebroventricular insulin administration in mice. Hippocampus 21, 1082–1092.
34. Hansen, M.B., Nielsen, S.E., and Berg, K. (1989). Re-examination and further development of a precise and rapid dye method for measuring cell growth/cell kill. J. Immunol. Methods 119, 203–210.
35. Szklarczyk, D., Morris, J.H., Cook, H., Kuhn, M., Wyder, S., Simonovic, M., Santos, A., Doncheva, N.T., Roth, A., Bork, P., Jensen, L.J., and von Mering, C. (2017). The STRING database in 2017: quality-controlled protein-protein association networks, made broadly accessible. Nucleic Acids Res. 45, D362–D368.
36. Franceschini, A., Szklarczyk, D., Frankild, S., Kuhn, M., Simonovic, M., Roth, A., Lin, J., Minguez, P., Bork, P., von Mering, C., and Jensen, L.J. (2013). STRING v9.1: protein-protein interaction networks, with increased coverage and integration. Nucleic Acids Res. 41, D808–D815.
37. Castro, M.A., Wang, X., Fletcher, M.N., Meyer, K.B., and Markowetz, F. (2012). RedeR: R/Bioconductor package for representing modular structures, nested networks and multiple levels of hierarchical associations. Genome Biol. 13, R29.
38. Israelsson, C., Kylberg, A., Bengtsson, H., Hillered, L., and Ebendal, T. (2014). Interacting chemokine signals regulate dendritic fells in acute brain injury. PLoS ONE. 9, e104754.
39. Davis, S. and Meltzer, P.S. (2007). GEOquery: a bridge between the Gene Expression Omnibus (GEO) and BioConductor. Bioinformatics 23, 1846–1847.

40. Ritchie, M.E., Phipson, B., Wu, D., Hu, Y., Law, C.W., Shi, W., and Smyth, G.K. (2015). limma powers differential expression analyses for RNA-sequencing and microarray studies. Nucleic Acids Res. 43, e47.
41. Figueira, T.R., Melo, D.R., Vercesi, A.E., and Castilho, R.F. (2012). Safranine as a fluorescent probe for the evaluation of mitochondrial membrane potential in isolated organelles and permeabilized cells. Methods Mol. Biol. 810, 103–117.
42. Johnson, V.E., Stewart, W., and Smith, D.H. (2013). Axonal pathology in traumatic brain injury. Exp. Neurol. 246, 35–43.
43. Perez-Pinzon, M.A., Stetler, R.A., and Fiskum, G. (2012). Novel mitochondrial targets for neuroprotection. J. Cereb. Blood Flow Metab. 32, 1362–1376.
44. DeWitt, D.S., Hawkins, B.E., Dixon, C.E., Kochanek, P.M., Armstead, W., Bass, C.R., Bramlett, H.M., Buki, A., Dietrich, W.D., Ferguson, A.R., Hall, E.D., Hayes, R.L., Hinds, S.R., LaPlaca, M.C., Long, J.B., Meaney, D.F., Mondello, S., Noble-Haeusslein, L.J., Poloyac, S.M., Prough, D.S., Robertson, C.S., Saatman, K.E., Shultz, S.R., Shear, D.A., Smith, D.H., Valadka, A.B., VandeVord, P., and Zhang, L. (2018). Pre-clinical testing of therapies for traumatic brain injury. J. Neurotrauma 35, 2737–2754.
45. Boyman, L., Williams, G.S., Khananshvili, D., Sekler, I., and Lederer, W.J. (2013). NCLX: the mitochondrial sodium calcium exchanger. J. Mol. Cell. Cardiol. 59, 205–213.
46. Kim, B. and Matsuoka, S. (2008). Cytoplasmic Na+-dependent modulation of mitochondrial Ca2+ via electrogenic mitochondrial Na+-Ca2+ exchange. J. Physiol. 586, 1683–1697.
47. Zhao, X., Gorin, F.A., Berman, R.F., and Lyeth, B.G. (2008). Differential hippocampal protection when blocking intracellular sodium and calcium entry during traumatic brain injury in rats. J. Neurotrauma 25, 1195–1205.
48. Giorgi, C., Agnoletto, C., Bononi, A., Bonora, M., De Marchi, E., Marchi, S., Missiroli, S., Patergnani, S., Poletti, F., Rimessi, A., Suski, J.M., Wieckowski, M.R., and Pinton, P. (2012). Mitochondrial calcium homeostasis as potential target for mitochondrial medicine. Mitochondrion 12, 77–85.
49. Jiang, D., Zhao, L., and Clapham, D.E. (2009). Genome-wide RNAi screen identifies Letm1 as a mitochondrial Ca2+/H+ antiporter. Science 326, 144–147.
50. Hill, R.L., Singh, I.N., Wang, J.A., and Hall, E.D. (2017). Time courses of post-injury mitochondrial oxidative damage and respiratory dysfunction and neuronal cytoskeletal degradation in a rat model of focal traumatic brain injury. Neurochem. Int. 111, 45–56.
51. Kulbe, J.R., Hill, R.L., Singh, I.N., Wang, J.A., and Hall, E.D. (2017). Synaptic mitochondria sustain more damage than non-synaptic mitochondria after traumatic brain injury and are protected by cyclosporine A. J. Neurotrauma 34, 1291–12301.
52. Ji, J., Kline, A.E., Amoscato, A., Arias, A.S., Sparvero, L.J., Tyurin, V.A., Tyurina, Y.Y., Fink, B., Manole, M.D., Puccio, A.M., Okonkwo, D.O., Cheng, J.P., Alexander, H., Clark, R.S., Kochanek, P.M., Wipf, P., Kagan, V.E., and Bayır, H. (2012). Lipidomics identifies cardiolipin oxidation as a mitochondrial target for redox therapy of acute brain injury. Nat. Neurosci. 15, 1407–1413.
53. Miller, D.M., Wang, J.A., Buchanan, A.K., and Hall, E.D. (2014). Temporal and spatial dynamics of nrf2-antioxidant response elements mediated gene targets in cortex and hippocampus after controlled cortical impact traumatic brain injury in mice. J. Neurotrauma. 31, 1194–1201.
54. Gardner, R., Salvador, A., and Moradas-Ferreira, P. (2002). Why does SOD overexpression sometimes enhance, sometimes decrease, hydrogen peroxide production? A minimalist explanation. Free Radic. Biol. Med. 32, 1351–1357.
55. Shahim, P., Tegner, Y., Wilson, D.H., Randall, J., Skillback, T., Pazooki, D., Kallberg, B., Blennow, K., and Zetterberg, H. (2014). Blood biomarkers for brain injury in concussed professional ice hockey players. JAMA Neurol. 71, 684–692.
56. Miller, D.M., Singh, I.N., Wang, J.A., and Hall, E.D. (2015). Nrf2-ARE activator carnosic acid decreases mitochondrial dysfunction, oxidative damage and neuronal cytoskeletal degradation following traumatic brain injury in mice. Exp. Neurol. 264, 103–110.
57. Zhang, Z., Larner, S.F., Liu, M.C., Zheng, W., Hayes, R.L., and Wang, K.K. (2009). Multiple alphaII-spectrin breakdown products distinguish calpain and caspase dominated necrotic and apoptotic cell death pathways. Apoptosis 14, 1289–1298.
58. Siman, R., Shahim, P., Tegner, Y., Blennow, K., Zetterberg, H., and Smith, D.H. (2015). Serum SNTF increases in concussed professional ice hockey players and relates to the severity of postconcussion symptoms. J. Neurotrauma 32, 1294–1300.
59. Saatman, K.E., Abai, B., Grosvenor, A., Vorwerk, C.K., Smith, D.H., and Meaney, D.F. (2003). Traumatic axonal injury results in biphasic calpain activation and retrograde transport impairment in mice. J. Cereb. Blood Flow Metab. 23, 34–42.
60. Toro-Urrego, N., Garcia-Segura, LM., Echeverria, V., and Barreto, G.E. (2016). Testosterone protects mitochondrial function and regulates neuroglobin expression in astrocytic cells exposed to glucose deprivation. Front. Aging Neurosci. 8, 152.
61. de la Fuente, A. (2010). From 'differential expression' to 'differential networking'—identification of dysfunctional regulatory networks in diseases. Trends Genet. 26, 326–333.

Address correspondence to:
Luis Valmor Portela, PhD
Department of Biochemistry
ICBS, UFRGS
Rua Ramiro Barcelos, 2600 anexo
90035-003, Porto Alegre, RS
Brazil

E-mail: roskaportela@gmail.com